A horizontal line in this figure would correspond to an $A^{\frac{2}{3}}$ dependence and the solid lines shown there indicate a dependence linear in A. It is apparent that the experimental points do lie between the limits defined by f_t and f_a. Furthermore the difference in A dependence for the π^+ and π^- cross sections, which is demonstrated in Fig. 1, is clearly predicted by the modified model employed here. Thus, although the particular A dependence of the data has not been calculated, the origin of the essential features has been shown.

ACKNOWLEDGMENTS

The author is indebted to Professor W. M. Woodward for suggesting the problem and for his help during the course of the experiment. He would like to thank Professor B. D. McDaniel for several constructive suggestions in the early phase of the work. Also, he would like to express his appreciation to the entire synchrotron staff whose combined efforts made this investigation possible.

PHYSICAL REVIEW VOLUME 123, NUMBER 4 AUGUST 15, 1961

Secondary Cosmic-Ray Photons below Cascade Energy*

KINSEY A. ANDERSON
Department of Physics, University of California, Berkeley, California
(Received April 7, 1961)

Investigations with small unshielded scintillation crystals carried through the atmosphere by balloons, show large fluxes of photons in the energy region 30 to 300 kev in equilibrium with the primary cosmic ray beam. At 90 g cm^{-2} depth the flux is about 22 photons cm^{-2} sec^{-1} compared with a charged particle flux determined from a Geiger tube of 1.9 cm^{-2} sec^{-1} at this same depth. The photon flux at zero depth, taken to be the albedo of this secondary cosmic-ray component, has been estimated by extrapolation to be 8 photons cm^{-2} sec^{-1} greater than 30 kev.

INTRODUCTION AND DESCRIPTION OF APPARATUS

ON a number of occasions during 1958 and 1959 scintillation spectrometers have been included in balloon borne payloads designed to study cosmic rays and auroral zone x-ray effects. Results from flights in the auroral zone, where frequent but sporadic influxes of x rays are occurring, have been published previously.[1,2] The purpose of the present discussion is to present some results concerning photons in the energy region 30 to 300 kev in equilibrium with the primary cosmic-ray beam and therefore always present in the atmosphere.

The experimental apparatus pertinent to the discussion is described in Table I. Scintillation counter data from only one balloon flight will be presented here, but several other flights have also led to the same results within experimental uncertainties involved in determining the atmospheric depth, the setting and stability of the discriminator edges, and the statistical fluctuations in the counting rates.

RESULTS

Figure 1 shows the ratio of the Geiger-Müller tube, counting rate to its geometry factor as a function of atmospheric depth. The detection efficiency of this tube for photons is less than $\frac{1}{2}\%$ at all energies, so that the ordinate of this plot represents very nearly the charged particle flux inside the cosmic-ray gondola assuming this flux to be isotropic over the upper hemisphere.

Figure 2 shows the counting rates in the four integral channels of the pulse-height analyzer divided by the geometry factor of the sodium iodide crystal determined from the same formula as the Geiger-Müller tube. The counting rate to geometry-factor ratio in the 34-kev channel of the scintillation counter is seen to be very much greater than that for the Geiger-Müller tube despite the fact that the crystal has a slightly thicker shielding. The crystal has an efficiency between 1 and 0.5 for detecting photons in the energy region 30 to 300 kev and unit efficiency for detecting charged particles entering its active region. From this it is concluded that the flux of photons must be much higher than the flux of charged particles at all depths in the atmosphere. This result is emphasized by Fig. 3.

To obtain the flux of photons present in the atmosphere (using the hemispherical geometry factor), two corrections have been applied to the scintillation counter data of Fig. 2. First, the charged particle flux as measured by the Geiger-Müller tube has been subtracted from all channels of the scintillation counter. This may be a slight overcorrection since the Geiger tube has a somewhat smaller wall thickness than the crystal. The analysis here uses results from a Geiger-Müller tube flown on a different day from the scintillation counter measurements. The Geiger-Müller tube was flown on August 4, while the scintillation counter measurements were taken on August 8, 1959. The Deep River neutron

* This work supported by the Office of Naval Research. It was a part of the U. S. participation in IGC 1959.
[1] K. A. Anderson, J. Geophys. Research **65**, 551 (1960).
[2] K. A. Anderson and D. C. Enemark, J. Geophys. Research **65**, 3521 (1960).

TABLE I. Description of the apparatus used to measure photons in the energy region 30 to 300 kev through the atmosphere.

Detector	Dimensions	Wall thickness[a]	Geometry factor	Depth of maximum rate in atmosphere
Geiger-Müller tube	Right cylinder 0.86 in. diam×3.7 in. high	0.035 g cm^{-2}	17.9 cm^2 [b]	50 g/cm^2
Scintillation crystal	Right cylinder 0.75 in. diam×0.75 in. high	0.13 g cm^{-2}	4.25 cm^2 [b]	100 g/cm^2
Twofold counter telescope	Tray dimensions: 1.72 in.×3.7 in. tray spacing: 4 in.	Particle range of 0.12 g cm^{-2} required for coincidence	12 cm^2 sr	90 g/cm^2

[a] In addition to the wall of the counters the apparatus is surrounded by an insulating gondola about 0.4 g cm^{-2} thick.
[b] Calculated from $\frac{1}{4}\pi a l(l+a/2l)$, where a is the diameter and l the height of the detector. This expression weights the counter area uniformly with respect to solid angle over the upper hemisphere.

monitor changes were less than 1% over this period and it is believed that comparison of counting rates on these two days leads to little or no error. The second correction is the efficiency for photoconversion of quanta incident on the crystal. Unit efficiency was used from 34 to 150 kev, $\epsilon=0.8$ from 150 to 300 kev, and $\epsilon=0.3$ for the >300-kev channel. Figure 4 shows the photon fluxes obtained in this manner.

The method used to obtain these efficiencies proceeds as follows. The integral photon spectrum cannot be unfolded with great reliability from the present measurements alone since the efficiency correction in the last integral channel is large and dependent on the spectral shape itself. Recent rocket measurements[3] carried out over Nevada, however, provide information on the photon spectrum in and above the atmosphere over the energy region 300 to 1000 kev. Using the spectral shape implied by these measurements of Northrop and Hostetler, a weighted efficiency for the crystal used in the present experiment is obtained for the 300-kev channel. This value is 0.3 giving a flux of 7.7 photons cm^{-2} sec^{-1} above 300 kev at the intensity maximum. This compares very well with the rocket measurement of 7.9 photons cm^{-2} sec^{-1} at the same depth and above the same energy threshold. This good agreement results despite the great difference in geomagnetic latitude between the rocket and balloon experiments because of the small latitude effect which existed at the time the measurements were made.

The ratio of crystal counting rate to geometry factor, corrected in the manner just described, is taken to be the flux of photons above the energies corresponding to the various discriminator settings. It is not certain how well

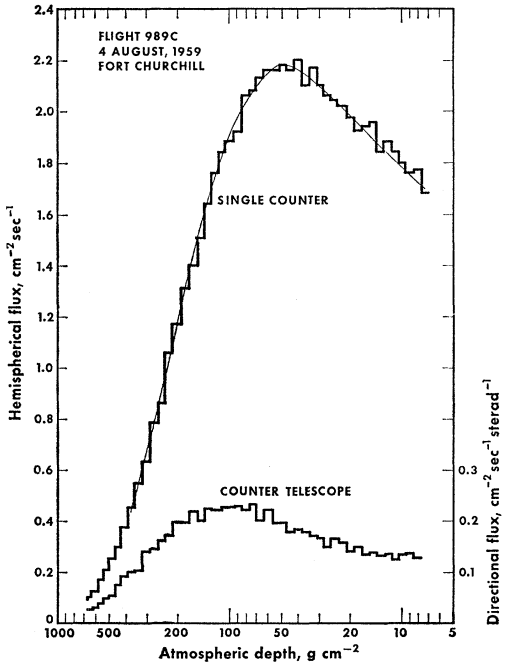

FIG. 1. The cosmic-ray flux through the atmosphere as measured by a thin-wall Geiger counter and a thin-wall counter telescope. August 4, 1959, was a quiet day during a time of high sunspot number.

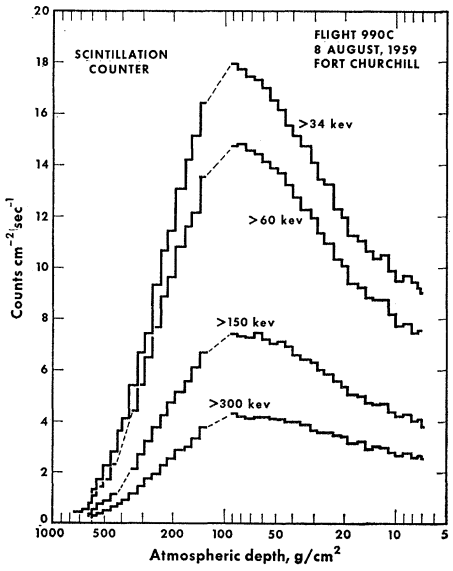

FIG. 2. The counting rate of a small scintillation crystal divided by its geometry factor. A transistorized pulse-height analyzer sorts the photomultiplier output into four integral channels.

[3] J. A. Northrop and R. L. Hostetler, Bull. Am. Phys. Soc. **6**, 52 (1961).

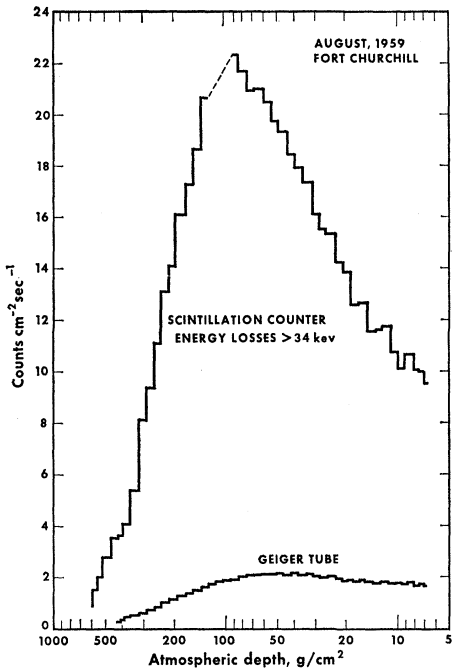

FIG. 3. The great abundance of low-energy photons in the atmosphere is seen by comparison of the scintillation counter and Geiger tube fluxes.

this ratio represents the true photon flux since the angular distribution of photons is unknown. One expects that from about 100 g/cm² upward, the peak of the angular distribution would be at a rather large zenith angle, with a considerable flux at 0° and a substantial contribution from the lower hemisphere due to the fact that these photons scatter readily. It is expected, however, that the spectral shapes to be derived here should not be far in error. The curves of Fig. 4 might be expected to include a spurious effect due to the fact that the high density of the crystal will induce a few nuclear interactions from incident neutrons. This effect would not be removed by the Geiger tube subtraction. Since the thickness of the crystal is about 6% of a nuclear free path this effect is probably not very large.

From the curves of Fig. 4, integral energy spectra can be obtained at any given atmospheric depth. Integral spectra are given in Fig. 5 for four different depths. The integral spectra are fitted fairly well by straight lines on a semilog plot and the best fits at the various depths are given in Table II. The general form of the integral This expression, where b and m are functions only of atmospheric depth, implies the following differential spectrum:

$$n(E)=m/E. \quad (2)$$

One expects the neutron contribution to disappear from the differential spectra since energy losses in these interactions should be the order of 1 Mev and therefore not appear in the differential energy spectra from 30 to

TABLE II. The integral photon flux can be fit rather well by an expression of the form $N(>E)=b-m\log_{10}E$. The quantities m and b, which are functions of atmospheric depth, are given above.

Atmospheric depth (g/cm²)	m	b
100	15	44.9
200	11.4	32.6
7	7.9	21.9
0	6.1	16.9

spectra is

$$N(>E)=b-m\log_{10}E, \quad 30<E<300 \text{ kev}. \quad (1)$$

300 kev. From Table II it can be seen that the spectrum falls most rapidly at 90 g/cm². The spectral form given above cannot hold much above 300 Mev since Northrop and Hostetler have shown a flux of photons having energies over 1000 kev.

It will be noticed in Fig. 5 that a spectrum has been plotted for zero atmospheric depth. This was derived by extrapolating the scintillation counter data to zero depth as shown in Fig. 6. Since the balloon reached a depth of 6.5 g cm^{-2} the extrapolation must be regarded as a quite reliable one. The main result of this extrapolation is that the flux of photons at zero depth is very large—about 8 cm^{-2} sec^{-1} above 30 kev.

DISCUSSION

(1) Figures 1 and 3 show that the intensity maximum for the low energy photons is much deeper in the

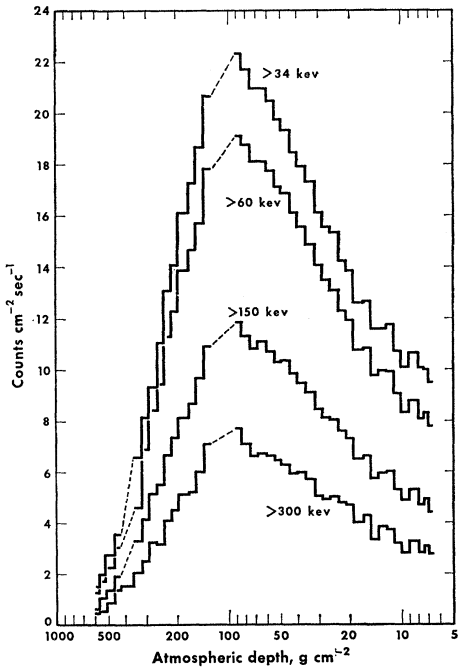

FIG. 4. The counting rate to geometry factor ratio in the four integral channels after corrections for photoelectric conversion and the charged-particle flux. The ordinate is thus interpreted as being the photon flux in the atmosphere averaged over the area of the scintillation crystal.

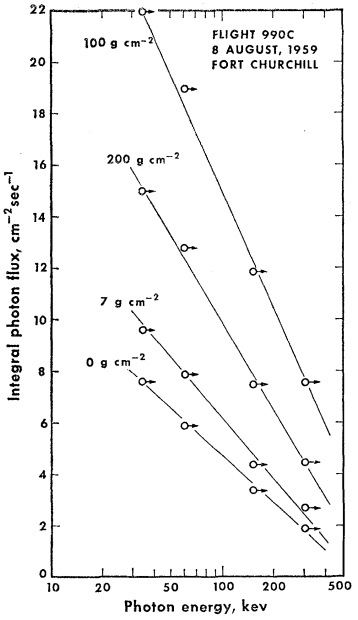

FIG. 5. Integral photon spectra at four atmospheric depths.

atmosphere than for the charged particles as measured by the Geiger tube. Interpreting the observed photons in the energy region 30 to 300 kev as degraded cascade shower photons, the location of their maximum at greater depth than the Geiger tube, which is responding strongly to the nucleonic cascade, follows from the fact that the electromagnetic cascade must "wait" for the nuclear interactions to provide the initiating π^0 mesons and the subsequent cascade development. Furthermore, the soft photons would be near the end of the average shower's development and this puts them even deeper into the atmosphere.

It is of interest to estimate the optimum thickness for the soft cascade photons. This can be done in an approximate way by comparison of the counter telescope, single counter and scintillation counter data. The counter telescope maximum is at 100 g cm^{-2} depth while the single counter transition occurs at 50 g cm^{-2}. This means that at 50 g cm^{-2} atmospheric depth the main contribution to the omnidirectional flux of charged particles is due to primaries that had a zenith angle of roughly 60° when entering the atmosphere. The directional flux of x rays from 0° zenith angle is not measured here but the same situation probably applies to the soft photons, namely that the original direction of the primaries responsible for the soft cascade photons is about 60° from the zenith. Since the single scintillation crystal shows a maximum at 100 g cm^{-2} the optimum thickness for the 30- to 300-kev photons is about 200 g cm^{-2}.

(2) The flux of photons in the energy region 30 to 300 kev in equilibrium with each high-energy photon in the cascade is very large. This can best be seen from Fig. 7 where the present data are combined with the rocket results of Northrop and Hostetler. The great abundance of soft photons is probably explained by the fact that when a photon has dropped below the pair threshold, the dominant means of interaction is the Compton process which scatters the photon many times before its energy is very much reduced. Below about 20 kev the photons should rather quickly disappear as photoelectric absorption becomes strong.

(3) The extrapolation to zero atmospheric depth shown in Fig. 6 gives the flux of the soft cascade photons at the top of the atmosphere. These must be interpreted as photons which are escaping from the earth. The photon albedo of the earth is seen from Fig. 6 to be large, being about 8 cm^{-2} sec^{-1} above 30 kev. Thus it is many times larger than the flux of charged particles entering the atmosphere as primary radiation. The Geiger tube flux extrapolated to zero depth 1.5 cm^{-2} sec^{-1} and includes the charged particle albedo as well as the primary contribution. Although the photon flux is high they represent a rather small energy flux. Evaluation of

$$\int_{30}^{300\text{ kev}} n(E)EdE$$

shows the total energy radiated away from the earth as photons of energy between 30 and 300 kev to be about 1700 kev/cm^2 sec. This is the order of 3×10^{-4} of the incoming primary cosmic-ray energy.

(4) The data presented here were obtained from balloon flights in the auroral zone but are not a unique feature of those latitudes. During 1959 there was little or no latitude effect at high altitude from Minneapolis up to the north dip pole. Therefore the fluxes and spectra obtained here apply over that range of latitude and possibly as far south as $\lambda=50°$N. Below this latitude the soft photon flux at all atmospheric depths would be expected to slowly decrease. The sporadic x-ray fluxes that frequently occur in the auroral zone do not contribute to the counting rates shown here. The auroral zone x rays have a much steeper spectrum and few photons above 150 kev are encountered. The auroral zone x-ray differential spectra vary about as E^{-4} while the soft cascade photons have a very flat spectrum going as E^{-1}.

(5) The experimental apparatus used was designed primarily to study the sporadically occurring auroral zone x rays which have intensities as high as 100 photons

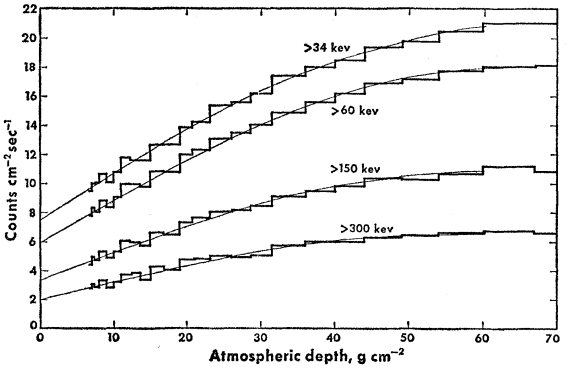

FIG. 6. Extrapolation of the counting rate to geometry factor ratio to zero atmospheric depth. The balloon flight attained 6.5 g cm^{-2}.

cm^{-2} sec^{-1} above 25 kev. Their average energy is also somewhat lower than the subcascade photons discussed here thus making a small crystal a desirable choice. The experimental results concerning the cascade photons could be improved by making the size of the scintillation crystal larger. A reduction in the size and uncertainty of the photoconversion efficiency correction and improvement in the statistical accuracy would improve knowledge of the flux versus depth curve including a better determination of the intensity maximum. Knowledge of the angular distribution of the photons would provide more accurate absolute flux values than those reported here. That measurement, however, would require a much more refined experiment than the present one which involves only a single unshielded crystal.

(6) Omnidirectional particle fluxes as determined from a thin-wall Geiger tube and the vertical directional fluxes from a thin-wall counter telescope have been reported here. These were determined during August of 1959, a time when solar activity was still generally high and the primary cosmic-ray flux depressed. The last Forbush decrease before the measurements occurred on July 18, and for about 5 days before the observation the Deep River neutron monitor was quite level. The flux values determined from the two counters as a function of atmospheric depth appear in Fig. 1.

(7) Although the results here are in general agreement with the rocket observations of Northrop and Hostetler, they do not seem to bear out results also obtained in rockets by Kuperian and Friedman[4] during 1955 at a geomagnetic latitude of 41°. In particular these workers find a well defined maximum in the differential photon energy spectrum at 100 kev when the rockoon system is floating at a depth of 35 g cm^{-2}. At this depth the present results do not reflect a corresponding marked flattening of the integral spectrum.

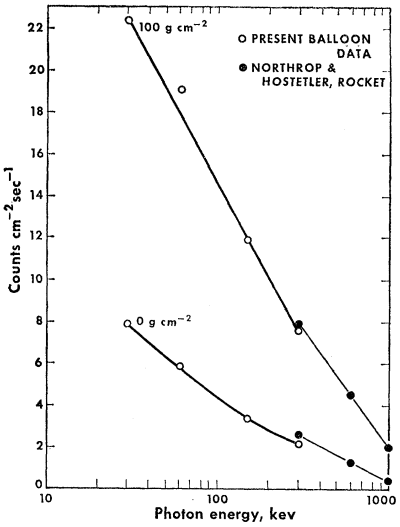

FIG. 7. Comparison of the present balloon results with rocket observations obtained by other workers.

[4] J. E. Kuperian, Jr., and H. Friedman, IGY Rocket Report Series, No. 1, 201 (1959).

PHYSICAL REVIEW VOLUME 123, NUMBER 4 AUGUST 15, 1961

Conversion of Muonium into Antimuonium*

G. FEINBERG†
Columbia University, New York, New York
AND
S. WEINBERG
University of California, Berkeley, California

(Received April 4, 1961)

A detailed analysis is made of the possible conversion of muonium into antimuonium in various environments. An assumed $\bar{\mu}e\bar{\mu}e$ weak interaction of the usual form and strength gives a probability of 2.5×10^{-5} in vacuum, even in the presence of reasonable external electric fields. In a solid the probability is less by at least 10, and probably 20, orders of magnitude. In an inert gas the probability is roughly to be divided by the numbers of collisions during a muon lifetime, and hence is quite small unless the pressure at room temperature is less than about 10^{-4} atm. Lowering the temperature does not help. A possible experiment is suggested.

I. INTRODUCTION

IT has been suggested[1,2] that muonium may be able to turn into antimuonium spontaneously. A specific example[3] of an interaction with this effect is

$$H=C\bar{\psi}_\mu\gamma_\lambda(1+\gamma_5)\Psi_e\bar{\psi}_\mu\gamma^\lambda(1+\gamma_5)\Psi_e, \quad (1)$$

which would yield a matrix element for conversion of $M(\equiv\mu^+e^-)$ into $\bar{M}(\equiv\mu^-e^+)$ equal to $\langle\bar{M}|H|M\rangle=\delta/2$,

* This work was supported in part by the U. S. Atomic Energy Commission and by the United States Air Force under a contract monitored by the Air Force Office of Scientific Research of the Air Research and Development Command and the Office of Naval Research.

† Alfred P. Sloan Foundation Fellow.

[1] B. Pontecorvo, Zhur. Eksp. i Teoret. Fiz. 33, 549 (1957).

[2] G. Feinberg and S. Weinberg, Phys. Rev. Letters 6, 381 (1961).

[3] S. L. Glashow [Phys. Rev. Letters 6, 196 (1961)] has remarked that only the charge-conjugation-invariant part of H can contribute to $\langle\bar{M}|H|M\rangle$, so that interactions may be constructed which forbid $M\to\bar{M}$ while allowing clashing beam reactions like $e^-+e^-\to\mu^-+\mu^-$. Such interactions have the property of conserving parity, if the relative $e-\mu$ parity is chosen imaginary; they allow $M\to\bar{M}$ if M has odd l, and $\bar{M}$ even l, or vice versa. The possibility of essentially imaginary relative parities can only arise when some quantum number (here, muon number) is multiplicatively conserved, as emphasized by G. Feinberg and S. Weinberg, Nuovo cimento 14, 571 (1959).